

Assimilation of remote sensing observations into a continuous distributed hydrological model: impacts on the hydrologic cycle

P. Laiolo¹, S. Gabellani¹, L. Campo¹, F. Silvestro¹, F. Delogu¹, R. Rudari¹, L. Pulvirenti^{1,2}, G. Boni¹, F. Fascetti², N. Pierdicca², R. Crapolicchio^{3,4}, S. Hasenauer⁵, S. Puca⁶

(1) CIMA Research Foundation, Savona, Italy

(2) Dept. Information Engineering, Electronics and Telecommunications, Sapienza University of Rome, Italy

(3) Serco SpA, Frascati, Italy;

(4) ESA-ESRIN, Frascati, Italy

(5) Department of Geodesy and Geoinformation, Vienna University of Technology, Vienna, Austria

(6) National Civil Protection Department, Rome, Italy

Corresponding author: Paola Laiolo, paola.laiolo@cimafoundation.org

1 Abstract

2 The reliable estimation of hydrological variables in space and time is of fundamental importance in
3 operational hydrology to improve the flood predictions. Nowadays remotely sensed data can offer a
4 chance to improve hydrological models especially in environments with scarce ground based data.
5 The aim of this work is to update the state variables of a physically based, distributed and
6 continuous hydrological model using four different satellite-derived data (three soil moisture
7 products and a Land Surface Temperature measurement) and one soil moisture analysis. The
8 experiments were carried out for a small catchment, in the northern part of Italy, for the period July
9 2012-June 2013. The products were pre-processed according to their own characteristics and then
10 they were assimilated into the model using a simple nudging technique. The benefits on the model
11 predictions of discharge were tested against observations. The analysis showed a general
12 improvement of the model discharge predictions for all the assimilation experiments, in particular
13 an added value to the model was found in the rainfall season (autumn). This demonstrated that a
14 distributed hydrological model, which works at fine scale resolution, can be ameliorated with the
15 assimilation of coarse-scale satellite-derive data using a careful data pre-processing and a simple
16 assimilation technique. The simplicity of this scheme makes it suitable to be applied in an
17 operational framework to simulate flood predictions.

18

1 **Keywords: satellite data assimilation; H-SAF; assimilation impacts; hydrological modelling;**
2 **soil moisture**

3 **1 Introduction**

4 Nowadays many fields of research and operational applications, such as agricultural production,
5 ecology, water resource management, rainfall-runoff prediction, weather/climate prediction and
6 disaster management require reliable estimation of hydrologic variables (Seneviratne et al., 2010).
7 Evapotranspiration, land surface temperature, soil moisture, snow water equivalent and others
8 hydrologic variables can be observed at ground, predicted by models and observed from space. In
9 particular, satellite observations related to land surface hydrological variables steadily increased in
10 the past decade in quantity and variety (Njoku et al., 2003; Bartalis et al., 2007; Clifford 2010;
11 Entekhabi et al., 2010; Gao et al., 2010; Kerr et al., 2010; Tedesco and Narvekar 2010; Foster et al.,
12 2011; Liu et al., 2011; Parinussa et al., 2012). However, all the estimates of hydrologic variables are
13 affected by errors and uncertainties: hydrological models suffer for uncertainties in model
14 initialization, model parameters, forcing and physics representations; satellite data often measure
15 indirect quantities and need forward models to retrieve hydrological variables; point measurements
16 are representative of very small areas on ground. To overcome these issues and produce a more
17 accurate hydrologic state estimation, different data-fusion and data assimilation techniques have
18 been developed (Walker and Houser 2005; Houser et al., 2010; Houser et al., 2012). Using data
19 assimilation techniques, satellite and/or ground observations can be merged into models to provide
20 hydrological estimates that are generally more accurate with respect to the observations or model
21 estimates alone (Liu et al., 2012). For more details about hydrologic data assimilation one may refer
22 to the review chapter in Houser et al., 2012. Examples of data assimilation in hydrologic
23 applications can be found for soil moisture (e.g. Houser et al., 1998; Pauwels et al., 2001; De
24 Lannoy et al., 2007; Drusch 2007; Reichle et al., 2007; Scipal et al., 2008; Crow and Ryu, 2009;
25 Draper et al., 2011; Brocca et al., 2012; Li et al., 2012; de Rosnay et al., 2012; Draper et al., 2012;
26 Han et al., 2012; Sahoo et al., 2013), surface temperature and snow cover (e.g. Liston and Hiemstra,
27 2008; Durand and Margulis, 2009; Kuchment et al., 2010; Reichle et al., 2010; Su et al., 2010;
28 DeChant and Moradkhani, 2011; De Lannoy et al., 2012). However the design and implementation
29 of a data assimilation scheme is still a research topic in hydrology, and it must be carefully
30 performed for several motivations (Reichle et al. 2013): (1) the spatial resolution of satellite-based
31 retrievals is usually much coarser than modelled one; (2) satellites observe electromagnetic
32 properties such as backscatter and/or radiances (or brightness temperatures) that are only indirectly
33 related to hydrological variables (Pierdicca et al., 2013a); (3) specific forward models and retrieval
34 algorithms need to be developed to convert satellite observations into measures of the hydrological

1 variable of interest (Pierdicca et al., 2014); (4) soil moisture satellite-observed backscatter and
2 radiances are sensitive to moisture in the top few centimetres of the soil, therefore information on
3 root zone soil moisture must be gathered. Regarding the assimilation of remotely sensed soil
4 moisture, most studies used land surface models or conceptual rainfall-runoff models (Weerts and
5 El Serafy, 2006; Crow and Ryu, 2009; Sahoo et al., 2013; Alvarez-Garreton et al 2014; Renzullo et
6 al., 2014); some of them explored the assimilation of satellite soil moisture estimates into physically
7 based hydrological models (Chen et al., 2011; Draper et al.,2011; Draper et al.,2012; Han et al.
8 2012; Flores et al. 2012; Wanders et al., 2014) and the most part of the studies used twin
9 experiments with synthetic data (e.g., Kumar et al., 2009; Crow and Ryu, 2009). Concerning
10 physically-based hydrological models, most of the soil moisture assimilation experiments on
11 distributed models have been conducted at regional or national scale using model spatial resolutions
12 at the order of 10 km or more (Draper et al., 2011; Daraper et al., 2012; Wanders et al., 2014); while
13 assimilations at small watershed scale have been applied mainly to semi-distributed model (Chen et
14 al., 2011; Han et al., 2012). Therefore, to our knowledge, there is still a lack of research on the use
15 of remotely sensed data within physically-based, distributed continuous hydrological models
16 working at spatial scales lesser than 1 km and applied to small basins (area less than 1000 km²). In
17 particular some questions and issues are still open: (1) the correct procedure to assimilate satellite
18 data (e.g. the definition of the observation operator and the bias handling), (3) how to face the
19 different resolutions of observations and models and (4) how to quantify the impact of data
20 assimilation on the hydrological cycle.

21 This work is devoted to the assimilation of four different soil moisture products (three derived from
22 ASCAT observations and one from SMOS mission) into the continuous, physically-based and
23 distributed model Continuum (Silvestro et al. 2013) applied to a small catchment in Italy. The
24 model is able to estimate, with a spatial resolution of 100 m, the soil moisture content over one
25 single soil layer which represents the root zone. An effort was made in order to define a simple and
26 robust pre-processing of satellite soil moisture data. Further experiments were the assimilation of
27 remotely sensed Land Surface Temperature (LST), as well as both LST and soil moisture
28 observations. Differently from other studies, which assimilated the hydrological variables using
29 mainly the Ensemble Kalman Filter, here a nudging technique was chosen in order to test if a
30 simple method is able to give improvements to the model performance. Moreover, the proposed
31 approach is computationally inexpensive making the procedure to be applied in an operational
32 framework to simulate flood predictions. The organization of this paper is as follows. Section 2
33 presents a description of the hydrological model used for the assimilation experiments in the test
34 basin. Section 3 describes the case study and the satellite-derived observations used for updating the

1 model; section 4 illustrates data pre-processing and the assimilation scheme; subsequent results are
2 presented in Section 5, whereas Section 6 provides the conclusions of the study.

3 **2 Continuum model overview**

4 Continuum is a continuous distributed physically based hydrological model able to reproduce the
5 spatial-temporal evolution of soil moisture, energy fluxes, surface soil temperature and
6 evapotranspiration. It was designed to find a balance between a detailed description of the physical
7 processes and a robust and parsimonious parameterization. The model solves the energy and mass
8 balance equations on a regular square mesh. Digital Elevation Model (DEM) and Land Cover Maps
9 are the only static data used to identify drainage network and soil parameters. Infiltration and
10 subsurface flow are described using a semi-empirical, but quite detailed, methodology based on a
11 modification of the Horton algorithm (Gabellani et al., 2008) and focused especially on exploiting
12 land use and climatology information to set the infiltration parameters. The surface flow
13 schematization distinguishes between channel and hill slope flow. The overland and channel flow
14 are described by a linear and a nonlinear reservoir schematization, respectively. The energy balance
15 is solved explicitly at cell scale by using the so called Force-Restore equation (Dickinson, 1988),
16 that allows the LST being considered as a distributed state variable of the model. The mass-balance
17 equations are integrated using a semi-implicit method (predictor-corrector scheme); vegetation
18 interception and water table flow are also simulated. A complete description of the model is
19 reported in Silvestro et al. (2013). Relevant for this study are the root zone saturation degree
20 (SD_{MOD}) and the Land Surface Temperature (LST_{MOD}) that are estimated by the model at the DEM¹
21 resolution (100 m) with an hourly time step. SD_{MOD} is the ratio between the actual water volume
22 and the maximum soil storage capacity. This latter is related to the soil type and land use through
23 the runoff curve number of the Soil Conservation Service (USDA Natural Resources Conservation
24 Service (NRCS), National Engineering Handbook, 2004) following Gabellani et al., 2008.

25 **3 The study area and the available satellite dataset**

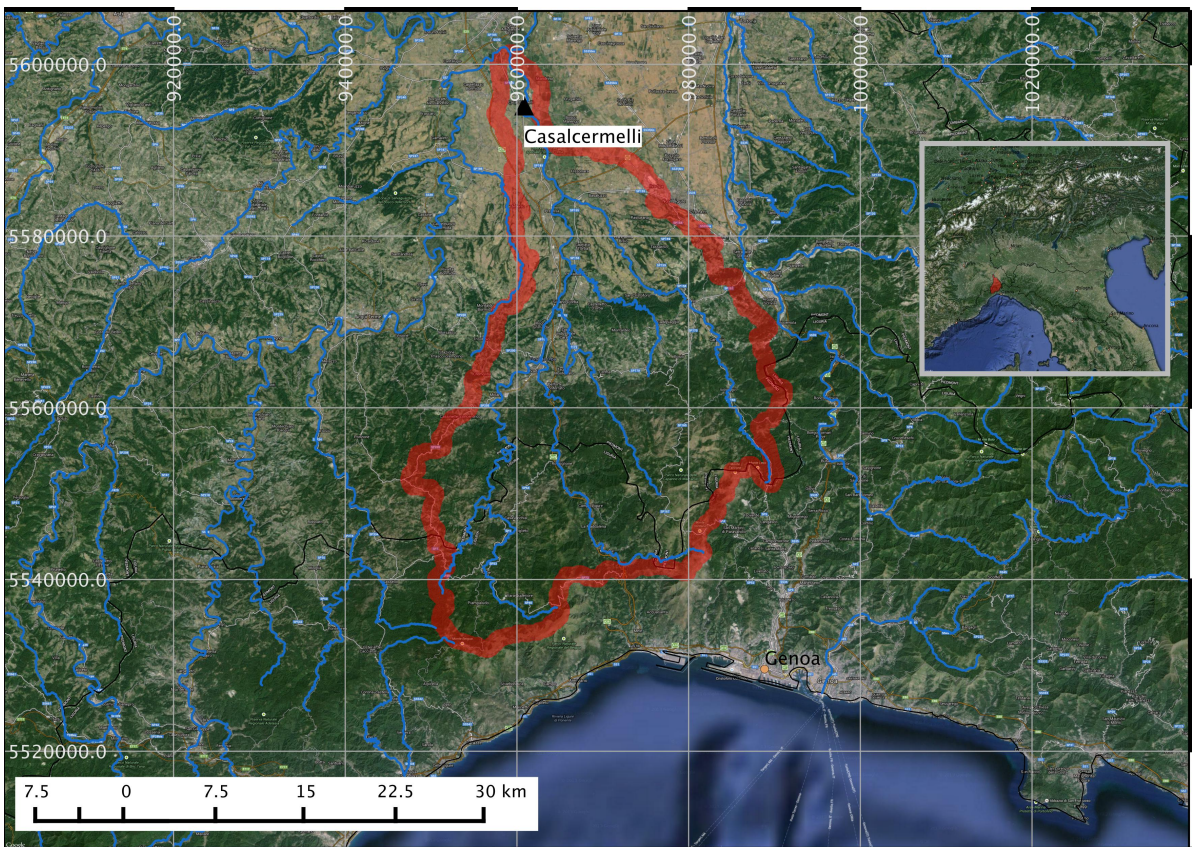
26 ***3.1 Study area: Orba watershed***

27 This study was conducted on the Orba basin that is located in the northern part of Italy (Figure 1)
28 and has an area of about 800 km². Orba River originates in Liguria region, and it flows through
29 Piemonte region reaching, near the city of Alessandria, the Bormida watercourse, which is one of
30 the tributaries of the Po river basin. The minimum and maximum elevations of the catchment are
31 106 m a.s.l. and 1280 m a.s.l., respectively, while the slope ranges from 0 in the flattest part to 90%
32 in the upper part of the basin. Almost the 50% of the basin is covered by forests (broadleaves and

¹ (http://www.igmi.org/prodotti/dati_numerici/dati_matrix.php)

1 coniferous), which are mainly present in the mountainous and hill areas of the catchment (at
2 elevations ranging from 500 m a.s.l. to 1280 m a.s.l.). Conversely, the flattest part of the Orba
3 catchment is mainly devoted to agriculture and cultivated forests (26% and 9%). Urban areas cover
4 only the 4% of the basin. The Orba River has mainly a rapid flow regime with recurrent flash floods
5 during autumn and spring and very low flows in summer. The Italian Civil Protection
6 meteorological network covers the catchment with 19 rain gauges, 19 thermometers, 10
7 hygrometers, 7 radiometers (shortwave), 8 anemometers and one level gauge (Casalcermeli)
8 located in the downstream part of the basin.

9



10

11

12

13

Figure 1 Location of Orba catchment. The blue lines represents the main river network of the considered area, while the red one represents the watershed

14

3.2 *Satellite dataset*

15

The analysed period started on July 1st 2012 and ended on June 30th 2013. Four different soil moisture products as well as a remotely sensed LST product were considered.

16

17

3.2.1 *Soil moisture products from H-SAF project*

18

Three soil moisture products used in this study were provided by the H-SAF project (<http://hsaf.meteoam.it/>), which generates, archives and validates high-quality satellite products for operational hydrology. These products were derived from the observations of the ASCAT sensor on

19

20

1 board of the EUMETSAT (European organization for the Exploitation of Meteorological Satellites)
2 polar orbiting Metop satellites. ASCAT is an active microwave sensor that provides global
3 backscatter measurements, at a resolution of 25 km, which are processed to surface soil moisture
4 (SSM) by using a change-detection method (Wagner et al. 2013). SSM represents the degree of
5 saturation of the topmost soil layer (0.5 - 2 cm) and it is given as an index ranging from 0 (dry) to
6 100 (wet). For the area of Western Europe, SSM measurements are available twice a day: one in the
7 morning (descending orbit) and one in the evening (ascending orbit). The ASCAT overpasses over
8 the Orba catchment are generally at 9.00 AM and at 8.00 PM. The H-SAF products considered in
9 this study are: 1) SM OBS 1 - H07 (large scale SSM) consists of maps of SSM over Europe and
10 North Africa with a spatial resolution of 25 km; 2) SM OBS 2 - H08 (small scale SSM) results
11 from disaggregating and re-sampling at 1 km the SM OBS 1 product; 3) SM DAS 2 - H14 (profile
12 index in the roots region) is a soil moisture analysis resulting from the assimilation of SM OBS 1
13 product into the ECMWF Land Data Assimilation System (de Rosnay et al., 2012). In this study
14 only the descending satellite passes was considered for H07 and H08 products. This because
15 previous studies on ASCAT-derived products (Wagner et al., 1999; Wagner et al., 2007; Albergel et
16 al., 2010) obtained better results using only those morning passes. H07 data are provided together
17 with four advisory flag indicating the probability to have: snow cover, frozen soil, complex
18 topography and wetland fraction. Moreover a quality flag, calculated as the maximum value of each
19 of the four advisory flags is supplied with the product. H14 product is provided as a soil moisture
20 index (from 0 to 1) at 00:00 UTC with a horizontal resolution of 25 km and at 4 depths: 0-7 cm, 7-
21 28 cm, 28-100 cm and 100-289 cm. In this study its weighted mean in the first two levels (0-7 cm
22 and 7-28 cm) was considered since this thickness is representative of the hydrological processes
23 modelled by Continuum in the root zone. From now on the term H14 will be referred as the mean of
24 the first two levels (0-28 cm).

25 ***3.2.2 Satellite soil moisture product from SMOS mission***

26 SMOS mission, launched in November 2009, is the ESA (European Space Agency) satellite
27 mission providing global observations of soil moisture over land and sea-surface salinity over the
28 oceans (Kerr et al., 2010). The measurements are derived from MIRAS (Microwave Imaging
29 Radiometer with Aperture Synthesis) passive microwave radiometer. The equator is crossed twice a
30 day: at 6 am (ascending or northward) and 6 pm (descending or southward) local time. This study
31 considered the Level 2 (L2) product that provides global maps of volumetric moisture content
32 (SMC) in the surface layer with a spatial resolution ranging from 35 km (centre of field of view) to
33 50 km (43 km average ground resolution). L2 data are sampled over the ISEA4h9 regular grid, with
34 15 km spacing. Only the ascending (dask) passes have been assimilated into the hydrological model

1 (Parrens et al., 2012) because evening measurements of passive microwaves sensors are strongly
2 affected by soil temperature effects, under these conditions the estimation of soil moisture could be
3 not accurate (Jackson, 1980; Gruhier et al., 2010). The L2 product is complemented by a Data
4 Quality index (DQX), an index related to the soil moisture retrieval uncertainty. It takes into
5 account the errors in the observations and it is provided in the volumetric soil moisture units.

6 ***3.2.3 Land Surface Temperature from LSA SAF***

7 The LST satellite observations used in this study were provided by LSA SAF (Satellite Application
8 Facility on Land Surface Analysis) of EUMETSAT (<http://landsaf.meteo.pt/>). The retrieval of LST
9 is based on clear-sky radiance measurements, in the thermal infrared window (channels IR10.8 and
10 IR12.0), from the Spinning Enhanced Visible and InfraRed Imager (SEVIRI) on EUMETSAT
11 geostationary Meteosat Second Generation (MSG) satellites. SEVIRI radiometer is orbiting above
12 the equator providing detailed imagery of Europe, the North Atlantic and Africa with a spatial
13 resolution of about 4.5 km. Theoretically, LST values can be determined 96 times per day (15
14 minutes temporal resolution); however, fewer observations are generally available due to cloud
15 cover contamination.

16 **4 Experiments setup**

17 ***4.1 Soil moisture data pre-processing***

18 Using a nearest neighbour approach, the satellite observations were interpolated from their native
19 resolutions to the 100 m Continuum grid (like in Draper et al., 2012). Then a quality control was
20 applied to each dataset according to the ancillary data provided with every product. No quality flags
21 are provided for H08 and H14 because the processor that generates them already masks data with
22 poor quality. Conversely, H07 data with quality, snow cover and frozen soil flags greater than 20
23 were discarded; no threshold was fixed for topographic complexity flag because its maximum value
24 over the Orba basin was found to be about 15%. Also SMOS data with quality index (DQX) greater
25 than 0.045 and Radio Frequency Interference probability (RFI) greater than 1% were not considered
26 (same thresholds used in Albergel et al., 2012 and Pierdicca et al., 2013b). Saturation degree
27 (SD_{MOD}) from Continuum is expressed as an index (between 0 and 1), while SMOS data have
28 volumetric soil moisture units. Hence, to make SMOS product comparable with SD_{MOD} , it was
29 normalized using its minimum and maximum values, as in Albergel et al., 2012, to obtain an index
30 ranging between 0 and 1. However, these satellite saturation degrees (SD_{OBS}), from H07, H08 and
31 SMOS, are referred to the first centimetres of soil while modelled data represent the water content
32 in the root zone, a deeper soil layer. To overcome this problem, the exponential filter developed by
33 Wagner et al. 1999 and modified by Albergel et al., 2008 (1) was adopted both for its simplicity and

1 for the request of a single parameter (T). This method allows to derive the Soil Water Index (SWI),
 2 i.e., a measure of saturation degree in the root zone which is comparable with SD_{MOD} .

$$3 \quad SWI_n = SWI_{n-1} + K_n (SD_{OBS}(t_n) - SWI_{n-1}) \quad (1)$$

4 Where K_n is the gain at time t_n (n is the time instant), which ranges between 0 and 1 and it is given
 5 by (2):

$$6 \quad K_n = \frac{K_{n-1}}{K_{n-1} + e^{-\left(\frac{t_n - t_{n-1}}{T}\right)}} \quad (2)$$

7 For the initialization of the filter, $K_1=1$ and $SWI_1=SD_{OBS}(t_1)$. The parameter T, named characteristic
 8 time length, characterizes the temporal variation of soil moisture within the root-zone profile. Since
 9 in situ soil moisture measurements are not available and the soil properties are not known
 10 quantitatively with high detail, the parameter T has been set to a priori value that has been estimated,
 11 as order of magnitude, using the definition of T of Wagner et al. 1999 and used also in Parajka et al.
 12 (2006) based on the mean soil characteristics of the considered catchment as described in the model
 13 (the average potential soil moisture capacity of the basin is 190 mm, assuming a porosity of 0.3, a
 14 pseudo diffusivity of 10 days would then translate into a wetting front celerity of 60 mm per day
 15 that is a typical value for these soil). Moreover, a value of T equal to 10 days is recommended by
 16 The Global Land Service (<http://land.copernicus.eu/global/?q=products/swi>). Then, to eliminate
 17 systematic biases between model and observations, the satellite data have been rescaled to model
 18 saturation degree climatology which was previously calculated over a period of two years. For SWI
 19 data (H07, H08 and SMOS) a rescaling between minimum and maximum value (3) was applied
 20 (Brocca et al., 2013) to obtain the rescaled SWI (SWI^*). This because the exponential filter smooths
 21 the time series and consequently reduces the variability range of SWI in a narrower range.

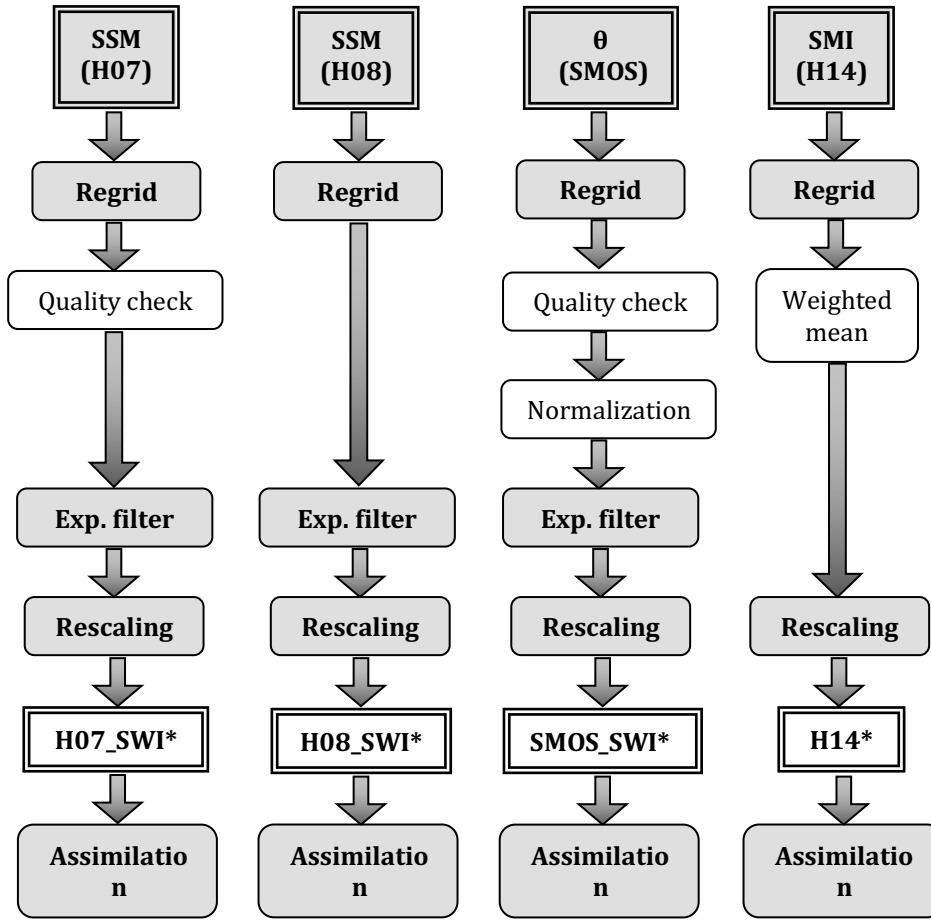
$$22 \quad SWI^* = \frac{SWI - \min(SWI)}{[\max(SWI) - \min(SWI)]} \cdot [\max(SD_{MOD}) - \min(SD_{MOD})] + \min(SD_{MOD}) \quad (3)$$

23 H14 product was processed in a different way as it is not directly derived from satellite surface
 24 observations but it is a model product which provides information about the soil moisture in the
 25 unsaturated zone. For this reason, only the rescaling to the model climatology was needed. The
 26 rescaled saturation degree from H14 ($H14^*$) was obtained using a linear rescaling technique (4)
 27 (Draper et al., 2009):

$$28 \quad H14^* = \frac{H14 - \mu(H14)}{\sigma(H14)} \cdot \sigma(SD_{MOD}) + \mu(SD_{MOD}) \quad (4)$$

29 Where μ and σ indicate the mean and standard deviation, respectively. The use of min-max
 30 correction for SWI and linear rescaling for H14 maximize the assimilation performances. The pre-

- 1 processing followed to elaborate each satellite-derived soil moisture product is shown in Figure 2.
 2 The rescaled products will be named hereinafter H07_SWI*, H08_SWI*, H14* and SMOS_SWI*.



3
 4 **Figure 2** The scheme indicates the methodology followed to pre-process the four soil moisture satellite data in
 5 order to assimilate them into Continuum model

6 **4.2 LST data pre-processing**

7 Due to the complex topography of the Orba basin, the LST satellite estimates cannot be directly
 8 assimilated into the model outputs because of the following problems: (1) the geometric registration
 9 of model and satellite pixels, (2) the shadowing due to the presence of mountains, and (3) the
 10 variation of the satellite viewing angle among different pixels due to sensor scanning geometry.
 11 These issues were solved applying a land model that projects the observed LST onto the geometry
 12 of the model (for detail see Silvestro et al. 2013). The land model produces a correlation matrix (**M**)
 13 that weights the model radiance to estimate the portion of energy of each model pixel that
 14 contributes to the energy of the satellite pixel. The application of the land surface model can be
 15 formalized as:

16
$$\varepsilon_{\text{mod}} LST_{\text{OBS}}^* = \mathbf{M} \cdot \varepsilon_{\text{obs}} LST_{\text{OBS}}^4 \quad (5)$$

1 Where LST_{OBS} is the satellite data, LST^*_{OBS} denotes the variable projected onto the model
 2 geometry, ϵ_{mod} and ϵ_{obs} are the model and satellite thermal emissivity. The model thermal emissivity
 3 is assumed constant, while ϵ_{obs} is estimated as the mean thermal emissivity of the two sensor
 4 channels used for LST-SAF retrieval.

5 **4.3 Assimilation scheme**

6 In this work, a simple nudging technique (Stauffer and Seaman, 1990; Brocca et al., 2010;
 7 Lakshminarayanan and Lewis, 2013) is employed for the assimilation of the remotely sensed variables
 8 into Continuum model. Although the nudging scheme is not optimal in a statistical sense, it is a
 9 computationally inexpensive approach to be applied in an operational framework to simulate flood
 10 predictions. The update was carried out only when the satellite data were available (once a day for
 11 soil moisture and hourly for LST as the higher update frequency) following this equation:

$$12 \quad X_{MOD}^+(t) = X_{MOD}^-(t) + G \cdot [X_{OBS}(t) - X_{MOD}^-(t)] \quad (6)$$

13 Where X_{MOD}^+ represents the updated modelled variable (X denotes LST or SD in case of LST or soil
 14 moisture assimilation), which was calculated by adding a “correction term” to the background-
 15 modelled variable (X_{MOD}^-). The correction term represents the difference between observed (X_{OBS})
 16 and modelled variable multiplied by a gain (G) that takes into account the uncertainties of both the
 17 model and the satellite observations. Pixels covered by urban areas and rivers were excluded from
 18 the assimilation experiments ($G=0$); while for the other points, G was estimated in different ways
 19 according to the type of assimilation. For soil moisture assimilation, G was calculated using the
 20 root mean square difference of both modelled ($RMSD_{MOD}$) and observed variable ($RMSD_{OBS}$):

$$21 \quad G = \frac{RMSD_{MOD}}{RMSD_{MOD} + RMSD_{OBS}} \quad (7)$$

22 $RMSD_{MOD}$ was assumed equal to 0.092 after performing a validation test in a different basin in
 23 which Continuum model outputs were compared with ground soil moisture measurements².
 24 $RMSD_{OBS}$ was considered equal to 0.22 for H14, 0.12 for both H07 and H08 and 0.24 for SMOS
 25 respectively (values obtained in Brocca et al., 2011; Albergel et al., 2012). Considering constant
 26 errors values over the time may lead to over-correction or under-correction of the model state if the
 27 actual errors are higher or lower with respect to the time-independent one. This problem could be
 28 achieved by estimating the RMSD, of both model and observations, in specific time windows
 29 depending on the meteorological or soil conditions. However, in an operational context these

² Soil moisture measurements from four TDR sensors located in Valle d’Aosta region (North-West Italy) were considered and compared with saturation degree modelled by Continuum model from January 2011 to December 2012.

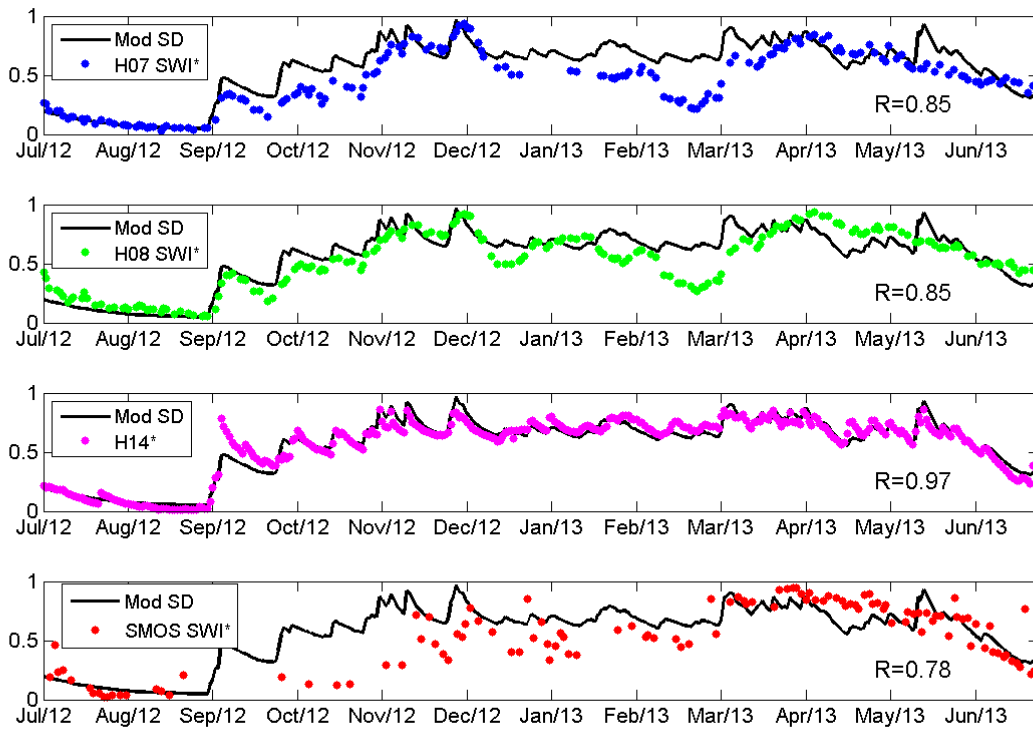
1 estimations become difficult since only past observations and model simulations are available. For
2 this reason constant error values were considered for each dataset in order to make the procedure
3 easily implemented. Moreover, for the same motivation, no spatial error correlation was considered
4 on the soil moisture products; however the rescaling process allows to spatialize the information at
5 each model grid taking into account the model climatology at model grid. The estimation of G for
6 the assimilation of LST followed a different strategy because LST ground measurements were not
7 available. The gain was varied between 0 and 1 and the value that maximized model performances
8 in terms of discharge prediction was chosen (like the procedure proposed in Brocca et al., 2010).
9 For LST assimilation G was then set equal to 0.4.

10 One assimilation experiment for each individual satellite-derived product was conducted;
11 furthermore, assimilations of LST jointly with each remotely sensed soil moisture product were also
12 attempted. A model run without assimilation (Open Loop – OL) was considered in order to verify
13 the impacts of each assimilation experiment (named with the suffix “Assim”). All the model runs
14 were initialized on June, 30 2012 using the state variables generated by OL simulations carried out
15 from June 2009. The parameters set was that obtained in Silvestro et al., 2013 after the calibration
16 of the model on the same catchment.

17 **5 Results**

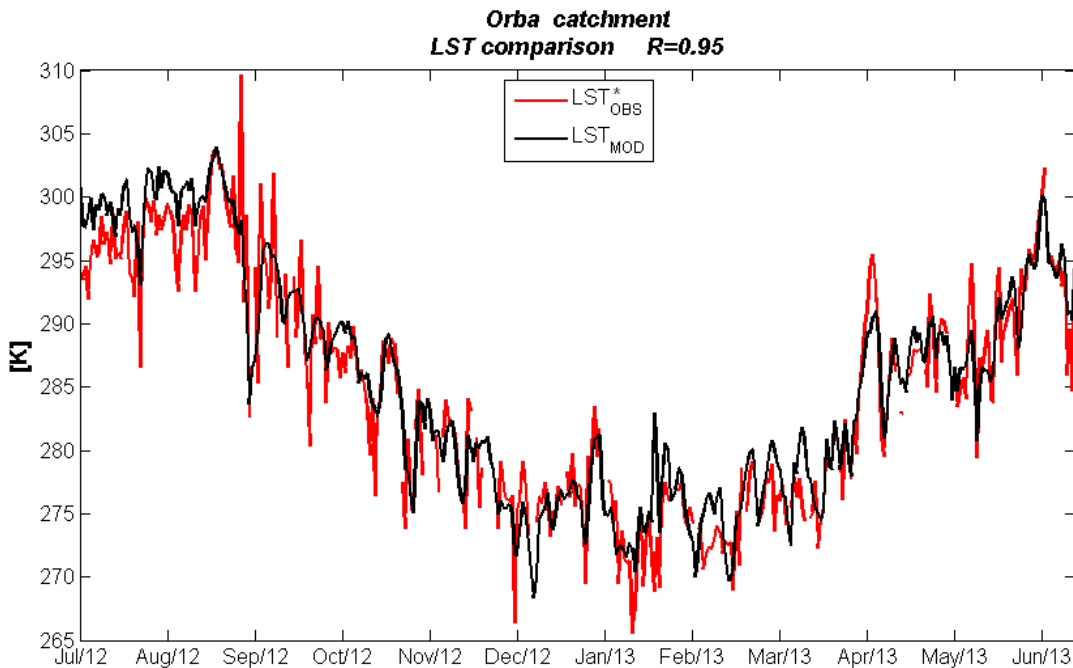
18 ***5.1 Variables comparisons at catchment scale***

19 Similarly to Brocca et al., 2012, before the assimilation experiments, the relationship between
20 satellite-derived observations and modelled quantities were investigated. The saturation degrees
21 derived from satellite data (H07_SWI*, H08_SWI*, H14* and SMOS_SWI*) and LST*_{OBS} were,
22 therefore, compared with OL simulations. The comparisons were done in terms of SD spatial
23 average at catchment scale (Figure 3) and catchment daily-averaged LST (Figure 4). The
24 correlations coefficients (R) were estimated and reported on each graph.



1
2
3
4

Figure 3 Comparison between model OL (black line) and satellite-derived soil moisture data (blue for H07_SWI*, green for H08_SWI*, magenta for H14* and red from SMOS_SWI*). The correlation coefficients are reported.



5
6
7
8

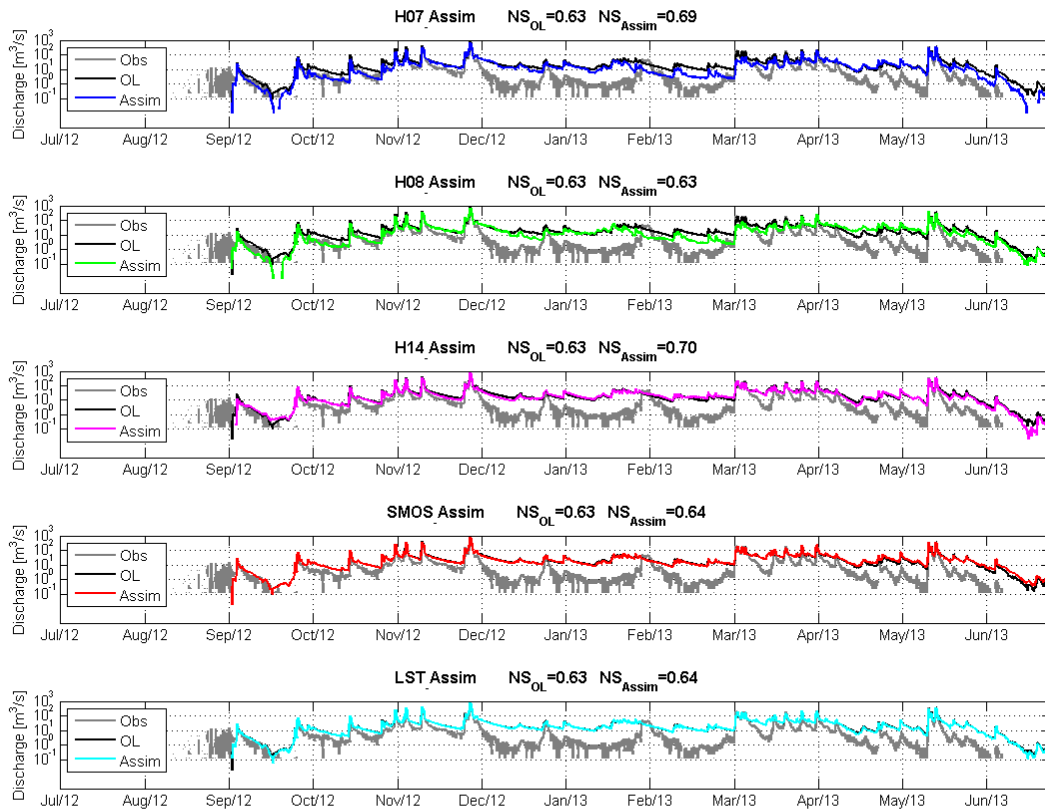
Figure 4 Comparison between OL modelled LST_{MOD} (black line) and LST^*_{OBS} (red line) land surface temperature. In the top of the graph the correlation coefficient is reported.

9 These results emphasized the good ability of all the soil moisture satellite products to reproduce the
 10 average saturation degree of the basin, indicating that they can be useful to assess soil moisture state
 11 on basins where in situ measurements are not available. The correlations between each series were
 12 high (R greater than 0.78), especially for H14*; LST^*_{OBS} also exhibited a high correlation with

1 model data. The graphs show that satellite products had some blanks; while H14 soil moisture
2 analysis data were always present (this product is daily derived from a land surface model). The
3 percentage of missing data was 69% for SMOS (mainly absent in autumn), 47% for H07 and 45%
4 for H08. Moreover, the masking process based on advisory flag allowed to exclude from the
5 experiment about the 6% of H07 maps in the winter period. ASCAT sensor has retrieval problems
6 in retrieving data in presence of frozen surfaces or snow cover; this is the reason of the
7 underestimation of soil moisture conditions with respect to the model in February 2013 for the
8 products H07 and H08. For LST satellite observations the percentage of missing data is 47%: most
9 of satellite images were unusable during autumn and spring due to cloud cover.

10 ***5.2 Assimilation experiments results***

11 The simulated discharges were compared to those observed by Casalcermelli level gauge in the
12 analysed period; evaluations were performed using the Nash–Sutcliffe model efficiency coefficient
13 (NS) (Nash and Sutcliffe, 1970), the root mean squared error (RMSE) and the mean absolute error
14 (MAE). H07_Assim and H08_Assim produced similar hydrographs (Figure 5) improving the
15 discharge estimation especially in the autumn period and underestimating the streamflow on
16 February 2013 (consequence of the dry soil moisture conditions showed on Figure 3). In general the
17 assimilations of H-SAF soil moisture products, in particular of H07_SWI* and H14*, improved the
18 efficiency of the model and reduced errors (Table 1). Conversely, SMOS_Assim and LST_Assim
19 lead to a weak improvement of model's performances. About SMOS this can be due to the few
20 SMOS data available over the catchment. The assimilations of both LST and soil moisture data
21 further reduced errors but did not altered the efficiency of the model (Table 1); consequently the
22 analyses that follow were done considering the single product assimilations only.



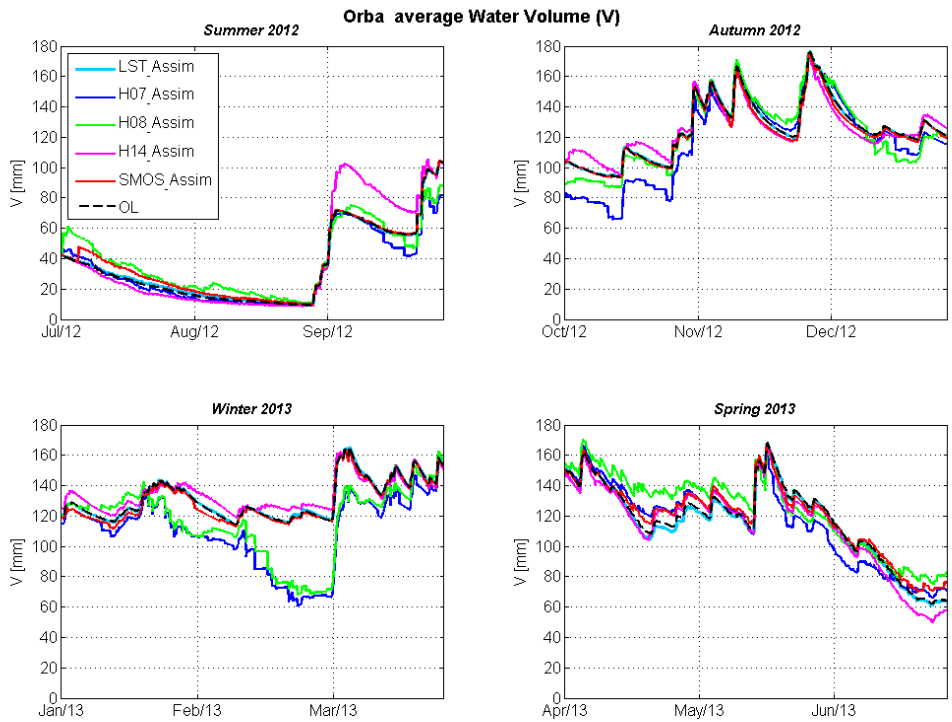
1
2 **Figure 5 Hydrographs, in logarithmic scale, from July 2012 to June 2013 at Casalcermelli outlet section.**
3 **Observed discharges (grey) and those from OL run (black) are compared with discharges resulting from**
4 **H07_Assim (blue), H08_Assim (green), H14_Assim (magenta), SMOS_Assim (red) and LST_Assim (cyan). On**
5 **the top of each graph the Nash-Sutcliffe coefficient of both OL and Assim case is reported**

6

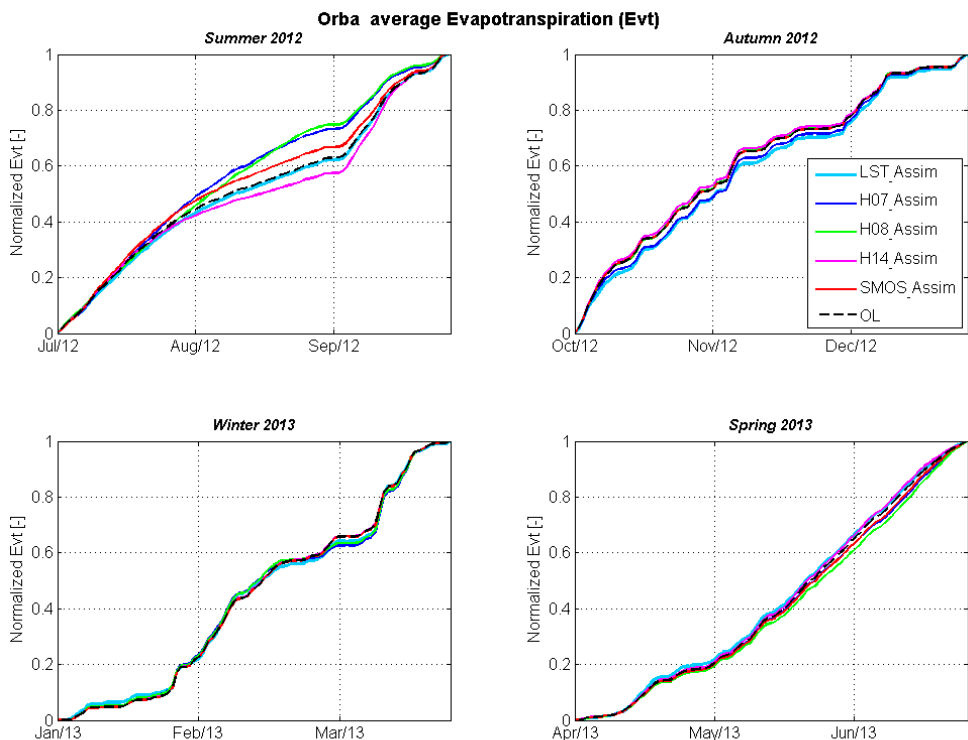
MAE, RMSE, NS – Annual analysis			
Experiment	MAE	RMSE	NS
OL	17.4	25.3	0.63
LST_Assim	17.1	25.0	0.64
H07_Assim	13.3	23.2	0.69
LST&H07_Assim	13.1	23.0	0.69
H08_Assim	15.5	25.4	0.63
LST&H08_Assim	15.3	25.2	0.63
H14_Assim	15.2	22.5	0.70
LST&H14_Assim	15.0	22.3	0.70
SMOS_Assim	17.5	25.0	0.64
LST&SMOS_Assim	17.1	24.6	0.65

7
8 **Table 1 MAE, RMSE and NS values calculated using simulated discharges resulting from different assimilation**
9 **runs with respect to the observed discharge**
10 Since in situ measurements of soil moisture, LST and evapotranspiration were not available on
11 Orba catchment, the impacts of model updates on the dynamics of these variables were evaluated
12 against the OL performance. In particular the changes of water volume (water content in the root

1 zone), normalized evapotranspiration and LST were analysed. Water volume (Figure 6) was the one
 2 mostly affected by soil moisture data assimilation. Significantly changes in the evapotranspiration
 3 (Figure 7) were recorded in summer; while LST (Figure 8) was not affected by soil moisture
 4 assimilations, but it was slightly modified by LST_Assim.

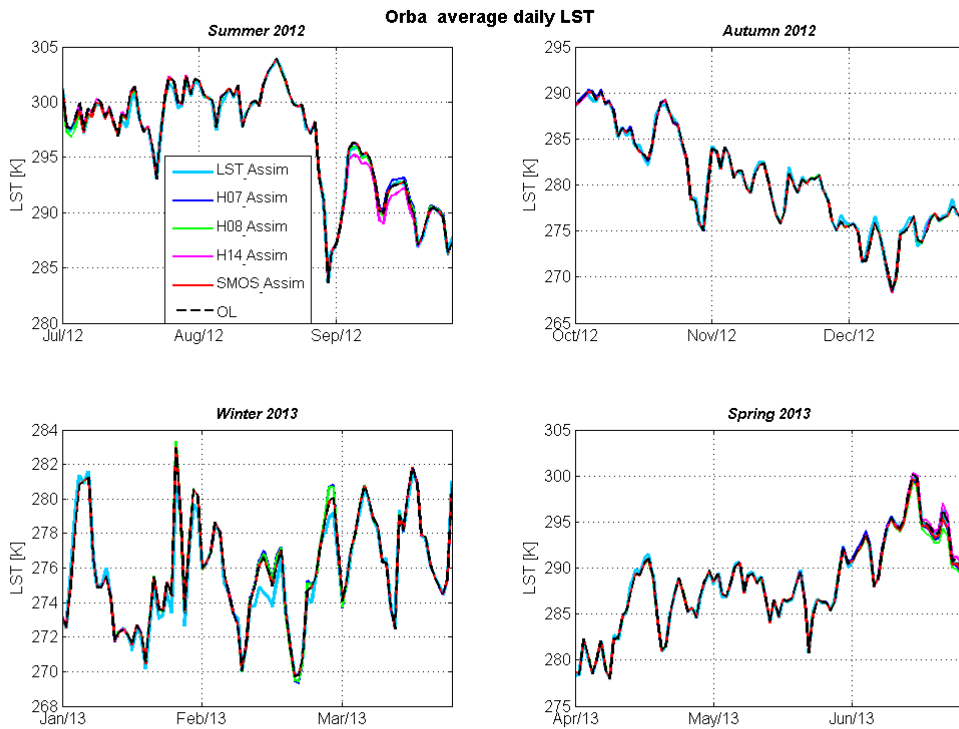


5
 6 **Figure 6** Catchment spatial averages of modelled water volume: OL (black dashed line), H07_Assim (blue),
 7 H08_Assim (green), H14_Assim (magenta), SMOS_Assim (red) and LST_Assim (cyan).
 8



9
 10 **Figure 7** Catchment spatial averages of modelled normalized evapotranspiration: OL model (black dashed line),
 11 H07_Assim (blue), H08_Assim (green), H14_Assim (magenta), SMOS_Assim (red) and LST_Assim (cyan).

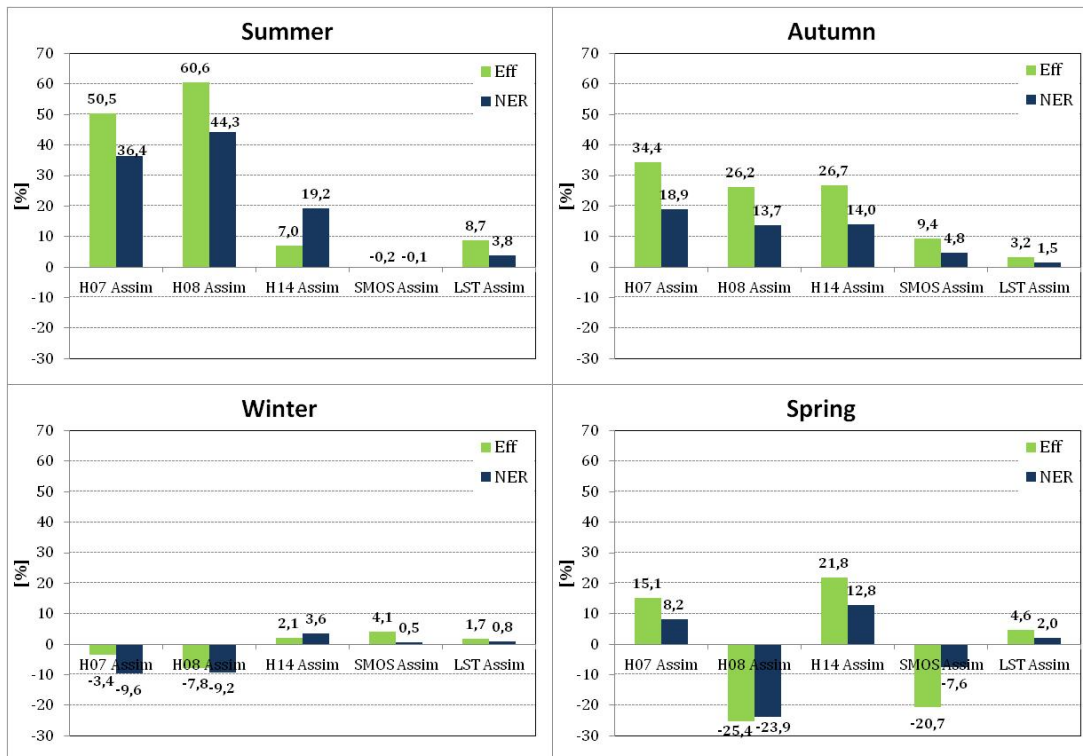
1
2



3
4
5
6

Figure 8 Catchment spatial averages of modelled LST: OL (black dashed line), H07_Assim (blue), H08_Assim (green), H14_Assim (magenta), SMOS_Assim (red) and LST_Assim (cyan).

7 Looking at the whole year period the results, in terms of statistical scores, of the assimilation
8 experiments are quite similar. For this reason, in order to better characterize the impact of the
9 assimilation on the discharge prediction, a seasonal analysis and an evaluation on eight selected
10 discharge events have been done. For these tests further statistical scores were used for the
11 evaluation: the Normalized Error Reduction (NER) (Chen et al., 2011) and the Efficiency of
12 assimilation (Eff) (Brocca et al., 2012). NER represents the percentage of reduction of RMSE with
13 respect to OL run, while Eff indicates the percentage of model efficiency improvement. A positive
14 value of these scores means that the assimilation gave an added value to the model. In summer
15 (Figure 8) the model performances were improved by all the assimilations except for SMOS_Assim
16 which didn't change the predictions. In particular H07_Assim and H08_Assim reduced mostly the
17 errors (Eff and NER greater than 35%); this probably was due to a better modelling of
18 evapotranspiration, which in summer was increased by H07_Assim and H08_Assim and decreased
19 by H14_Assim. In autumn all the assimilations, especially those relative to H-SAF products,
20 improved the model. While in winter H07_Assim and H08_Assim reduced the model's efficiency
21 with respect to OL run: due to the ASCAT retrieval problems explained above, the soil moisture
22 and consequently the discharge were underestimated. H14_Assim and H07_Assim were the only
23 experiments, which gave significant improvements to Continuum in spring.



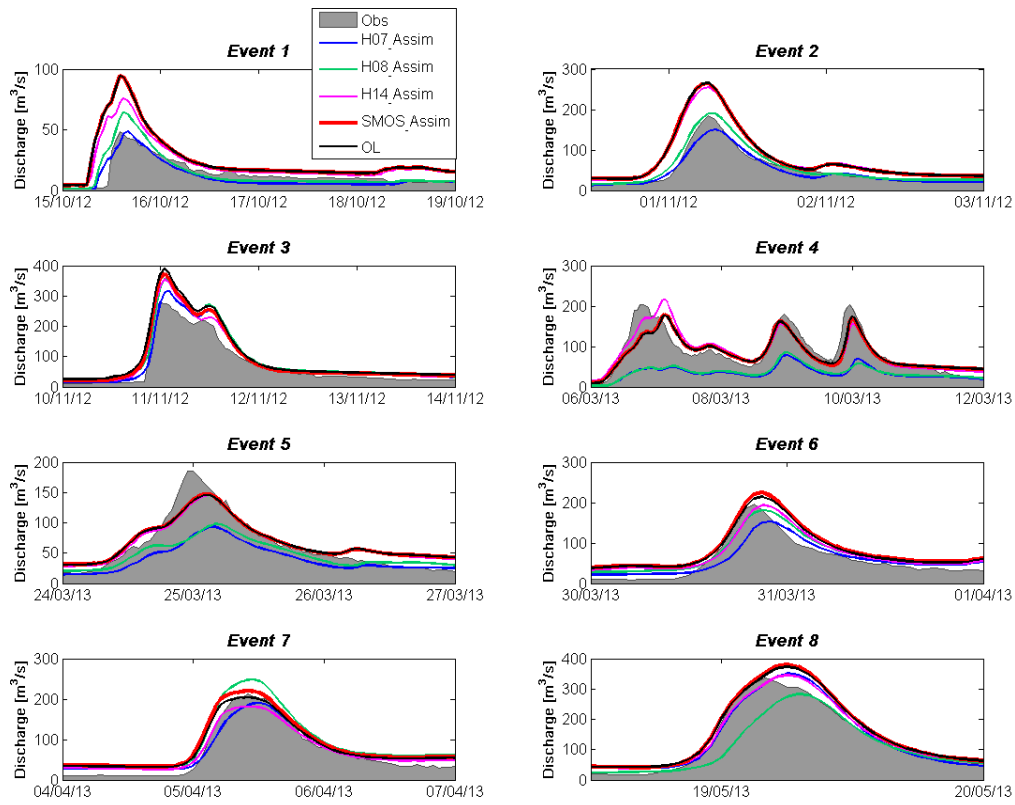
1

2 **Figure 9** The histograms reports, for each season, the Eff (green) and NER (blue) values resulting from each
 3 assimilation experiment. The numbers above each column indicate the values of these scores.

4

5 Eight events (three in autumn, one in winter and four in spring), with observed discharge greater
 6 than 50 m³/s, were selected in the analysed period (Figure 10). This analysis was done considering
 7 only the soil moisture assimilation experiments and calculating Eff and NER coefficients (Figure
 8 11). The assimilation of SMOS product was able to improve only one event (Ev.3) out of eight,
 9 H08_Assim increased the performance of four events, while the other two experiments improved
 10 most of the events (six for H07_Assim and seven for H14_Assim). Model predictions on autumn
 11 events (Ev.1, Ev.2 and Ev.3) were improved by all the H-SAF products. In particular, Ev.1 and Ev.2
 12 were significantly improved by H07_Assim and H08_Assim with Eff and NER greater than 60%.
 13 During winter events (Ev.4 and Ev. 5) the assimilations did not improve the performances because
 14 Eff and NER were below or near zero; moreover, the ASCAT problems in winter are evident by
 15 looking at the scores relative to H07_Assim and H08_Assim. Like in seasonal analysis, H14_Assim
 16 and H07_Assim lead to very good improvements for the last three events occurred in spring (Ev.6,
 17 Ev.7 and Ev.8). Looking at the seasonal and event analysis some differences among the results of
 18 each assimilation experiment can be seen. The assimilation of H14 soil moisture analysis always
 19 improved the model indicating that such a product, derived in turn by another model simulation, is
 20 able to correct the soil moisture status. Conversely, H07 and H08 Assim helped to increase the
 21 performances only in some period of the year. Moreover the benefits given by these two
 22 assimilations in autumn events are higher with respect to the H14_Assim ones.

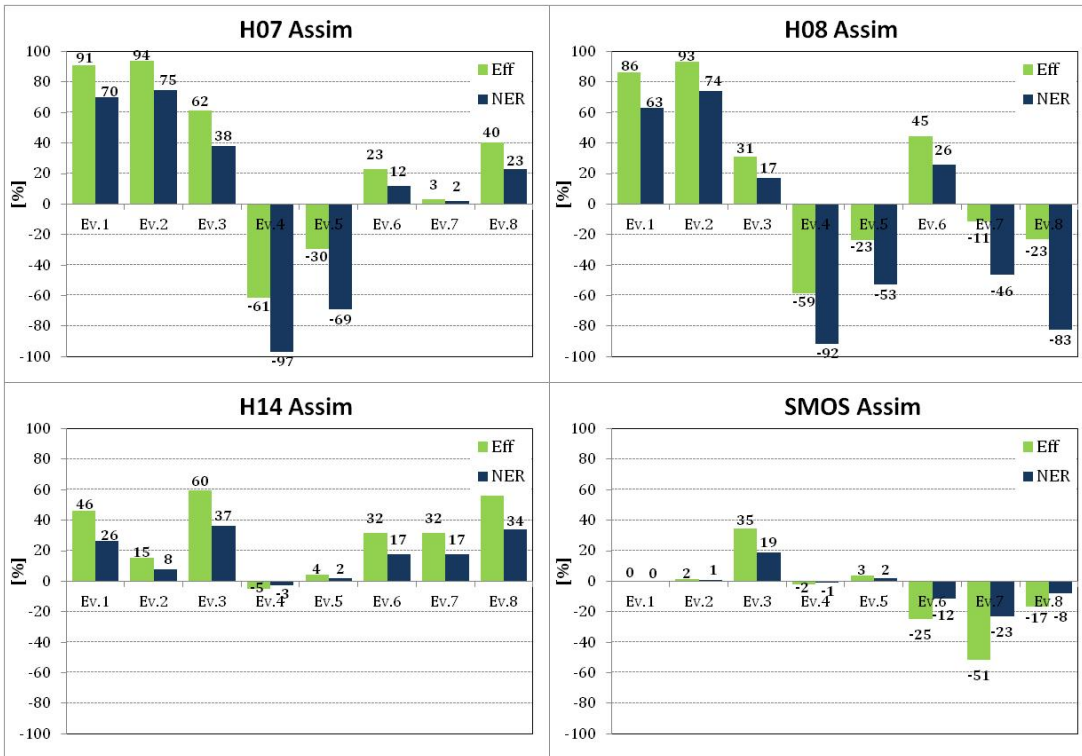
1



2

3 **Figure 10 Hydrographs for eight different events. The graphs show observed discharges (grey dashed lines), OL**
 4 **(black), H07_Assim (blue), H08_Assim (green), H14_Assim (magenta), SMOS_Assim (red) and LST_Assim**
 5 **(cyan)**

6



7

1 **Figure 11 The histograms reports, for each assimilation experiment, the Eff (green) and NER (blue) values**
2 **resulting relative to the eight selected discharge events. The numbers above each column indicate the values of**
3 **these scores.**

4 **6 Conclusions**

5 This work was devoted to the investigation of the impact of the assimilation of different remote
6 sensing products into a continuous distributed hydrological model. Four different satellite-derived
7 soil moisture products, as well as LST observations, were considered. Three soil moisture products
8 are distributed within the EUMETSAT H-SAF project, while SMOS mission provides the fourth.
9 LST measurements were retrieved from MSG satellites. Particular attention have been paid to the
10 pre-processing of these products, taking into account the characteristics of the considered basin
11 (elevation, land cover, river network), the satellite retrieval problems (snow and frozen surfaces,
12 topographic complexity) and the model peculiarities (space and time step and variables
13 climatology). Then each single satellite-derived product was assimilated into the hydrological
14 model using a nudging technique. Analysis on the impact of assimilations over the hydrological
15 cycle revealed that the variable most affected by the assimilation of satellite-derived soil moisture
16 data is the soil water volume; while land surface temperature was poorly modified by assimilations
17 and changes in evapotranspiration occurred only in the warmest season. Results of assimilation
18 experiments were assessed in terms of discharge comparing the model predictions to the data
19 observed by a selected gauge using different statistical scores. The evaluations showed a general
20 improvement of the model predictions for all the assimilation experiments; in particular an added
21 value to the model was found in the estimation of discharge events happened in the heavy rainfall
22 season (autumn). The discharge predictions were mainly enhanced by soil moisture updates;
23 however evenly the assimilation of LST product was able to reduce the errors. This work has
24 demonstrated that remotely sensed data could be used to update a physically-based, distributed
25 hydrological model applied to a small catchment using a careful data elaboration and a simple DA
26 technique which is easy to be applied for Civil Protection purposes in an operative flood forecasting
27 framework. Moreover, the positive results of the assimilation experiments allow to conclude that,
28 similarly to what found in Wanders et al., 2014, satellite data could be used to improve the model
29 performance for ungauged basins. This DA procedure has been tested over a Mediterranean
30 catchment located in the Italian Apennines and Po Valley; anyhow, it should be tested over different
31 environments such as in regions where satellite data may have some troubles in the soil moisture
32 retrieval related to complex topography or snow cover, like Italian Alps. In these regions an added
33 value to the assimilation process could be given avoiding the soil moisture update when the
34 modeled land surface temperature is below zero or where snow cover is observed by snow gauges.
35 Therefore we recommend that efforts should be focused on ensuring adequate data pre-processing

1 considering the characteristics of the considered region and the peculiarities of both satellite
2 products and hydrological model.

3 **Acknowledgements**

4 This work was supported by the Italian Civil Protection Department and by the Italian Regions of
5 Valle d'Aosta and Liguria. The authors thank the H-SAF project for providing soil moisture data
6 derived from ASCAT observations. SMOS L2 data have been gathered within the framework of an
7 ESA category-1 project.

8 **7 References**

9 Albergel, C., Rüdiger, C., Pellarin, T., Calvet, J. C., Fritz, N., Froissard, F., Suquia, D., Petitpa, A.,
10 Piguet, B., & Martin, E., 2008. From near-surface to root-zone soil moisture using an exponential
11 filter: An assessment of the method based on in-situ observations and model simulations.
12 *Hydrology and Earth System Sciences*, 12, 1323–1337. DOI:10.5194/hess-12-1323-2008.

13 Albergel, C., Calvet, J.-C., de Rosnay, P., Balsamo, G., Wagner, W., Hasenauer, S., Naeimi, V.,
14 Martin, E., Bazile, E., Bouyssel, F., and Mahfouf, J.-F., 2010. Cross-evaluation of modelled and
15 remotely sensed surface soil moisture with in situ data in southwestern France, *Hydrol. Earth Syst.*
16 *Sci.*, 14, 2177–2191, doi:10.5194/hess-14-2177-2010.

17 Albergel, C., de Rosnay, P., Gruhier, C., Muñoz-Sabater, J., Hasenauer, S., Isaksen, L., Kerr, Y.,
18 and Wagner, W., 2012. Evaluation of remotely sensed and modelled soil moisture products using
19 global ground-based in situ observations. *Remote Sens. Environ.*, vol. 118, pp. 215-226.

20 Alvarez-Garreton, C., Ryu, D., Western, A. W., Su, C.-H., Crow, W. T., Robertson, D. E., and
21 Leahy, C.: Improving operational flood ensemble prediction by the assimilation of satellite soil
22 moisture: comparison between lumped and semi-distributed schemes, *Hydrol. Earth Syst. Sci.*
23 *Discuss.*, 11, 10635-10681, doi:10.5194/hessd-11-10635-2014, 2014.

24 Bartalis, Z., Wagner, W., Naeimi, V., Hasenauer, S., Scipal, K., Bonekamp, H., Figa, J., C.
25 Anderson, C., 2007. Initial soil moisture retrievals from the METOP-A Advanced Scatterometer
26 (ASCAT). – *Geophys. Res. Lett.*, 34, l20401.

27 Brocca, L., Melone, F., Moramarco, T., Wagner, W., Naeimi, V., Bartalis, Z., and Hasenauer, S.
28 (2010). Improving runoff prediction through the assimilation of the ASCAT soil moisture product,
29 *Hydrol. Earth Syst. Sci.*, 14, 1881–1893, doi:10.5194/hess-14-1881-2010.

1 Brocca, L., Hasenauer, S., Lacava, T., Melone, F., Moramarco, T., Wagner, W., Dorigo, W.,
2 Matgen, P., Martínez-Fernández, J., Llorens, P., Latron, J., Martin, C., Bittelli, M., 2011. Soil
3 moisture estimation through ASCAT and AMSR-E sensors: an intercomparison and validation
4 study across Europe. *Remote Sensing of Environment*, 115, 3390-3408,
5 doi:10.1016/j.rse.2011.08.003. <http://dx.doi.org/10.1016/j.rse.2011.08.003>.

6 Brocca, L., Moramarco, T., Melone, F., Wagner, W., Hasenauer, S., and Hahn, S., 2012.
7 Assimilation of surface- and root-zone ASCAT soil moisture products into rainfall runoff modeling,
8 *IEEE T. Geosci. Remote*, 50, 2534–2555, doi:10.1109/TGRS.2011.2177468.

9 Brocca, L., Melone, F., Moramarco, T., Wagner, W., Albergel, C., 2013. Scaling and filtering
10 approaches for the use of satellite soil moisture observations, in: "Remote Sensing of Land Surface
11 Turbulent Fluxes and Soil Surface moisture Content: State of the Art". Taylor & Francis Ed,
12 Chapter 17, pp. 415-430.

13 Chen, F., Crow, W.T., Starks, P.J., Moriasi, D.N., 2011. Improving hydrologic predictions of a
14 catchment model via assimilation of surface soil moisture. *Advances in Water Resources* 34 (4),
15 526–536.

16 Clifford, D., 2010. Global estimates of snow water equivalent from passive microwave instruments:
17 history, challenges, and future developments. *Int J Remote Sens* 31:3707–3726.

18 Crow, W. T. and Ryu, D., 2009. A new data assimilation approach for improving runoff prediction
19 using remotely-sensed soil moisture retrievals, *Hydrol. Earth Syst. Sci.*, 13, 1–16, doi:10.5194/hess-
20 13-1-2009.

21 DeChant, C. M. and Moradkhani, H., 2011. Radiance data assimilation for operational snow and
22 streamflow forecasting, *Adv. Water Resour. Res.*, 34, 351–364.

23 De Lannoy, G. J. M., Reichle, R. H., Houser, P. R., Pauwels, V. R., and Verhoest, N. E., 2007.
24 Correcting for forecast bias in soil moisture assimilation with the ensemble Kalman filter, *Water*
25 *Resour. Res.*, 43, W09410, doi:10.1029/2006WR005449.

26 De Lannoy, G. J. M., Reichle, R. H., Arsenault, K. R., Houser, P. R., Kumar, S., Verhoest, N. E. C.,
27 and Pauwels, V. R. N., 2012. Multiscale assimilation of Advanced Microwave Scanning
28 Radiometer. EOS snow water equivalent and Moderate Resolution Imaging Spectro radiometer
29 snow cover fraction observations in northern Colorado, *Water Resour. Res.*, 48, W01522,
30 doi:10.1029/2011WR010588.

- 1 de Rosnay, P., Drusch, M., Vasiljevic, D., Balsamo, G., Albergel, C., Isaksen, L., 2012. A
2 simplified extended Kalman filter for the global operational soil moisture analysis at ECMWF. Q J
3 R Meteorol Soc. doi:10.1002/qj.2023.
- 4 Dickinson, R., 1988. The force-restore method for surface temperature and its generalization,
5 Journal of Climate, 1:1086-1097.
- 6 Draper, C., Walker, J.P., Steinle, P., De Jeu, R.A.M., Holmes, T.R.H., 2009. An evaluation
7 of AMSR-E derived soil moisture over Australia. Remote Sensing of Environment, 113 (4),703-
8 710.
- 9 Draper, C.S., Mahfouf, J.-F., Calvet, J.-C., Martin, E., Wagner, W., 2011. Assimilation of ASCAT
10 near-surface soil moisture into the French SIM hydrological model. Hydrol. Earth Syst.
11 Sci. 15: 3829–3841, DOI: 10.5194/hess-15-3829-2011.
- 12 Draper, C.S., Reichle, R.H., De Lannoy, G.J.M., Liu, Q., 2012. Assimilation of passive and active
13 microwave soil moisture retrievals. Geophys Res Lett 39:L04401. doi:10.1029/2011GL050655.
- 14 Drusch, M., 2007. Initializing numerical weather prediction models with satellite derived surface
15 soil moisture: data assimilation experiments with ECMWF's Integrated Forecast System and the
16 TMI soil moisture data set. J Geophys Res 112:D03102. doi:10.1029/2006JD007478.
- 17 Durand, M., Kim, E. J., and Margulis, S. A., 2009. Radiance assimilation shows promise for
18 snowpack characterization, Geophys. Res. Lett., 36, L02503, doi:10.1029/2008GL035214, 2009.
- 19 Entekhabi, D., Njoku, E. G., O'Neill, P. E., Kellogg, K. H., Crow, W. T., Edelstein, W. N., Entin, J.
20 K., Goodman, S. D., Jackson, T. J., Johnson, J., Kimball, J., Piepmeier, J. R., Koster, R. D., Martin,
21 N., McDonald, K. C., Moghaddam, M., Moran, S., Reichle, R., Shi, J. C., Spencer, M. W., Thurman,
22 S. W., Leung T., Zyl, J., 2010. The Soil Moisture Active Passive (SMAP) Mission, Proceedings of
23 the IEEE, 98, 704–716, doi:10.1109/JPROC.2010.2043918.
- 24 Flores, A. N., Bras, R. L., and Entekhabi, D., 2012. Hydrologic data assimilation with a hillslope-
25 scale-resolving model and L band radar observations: Synthetic experiments with the ensemble
26 Kalman filter, Water Resour. Res., 48, W08509, doi:10.1029/2011WR011500.
- 27 Foster, J.L., Hall, D.K., Eylander, J.B., Riggs, G.A., Nghiem, S.V., Tedesco, M. Kima, E.,
28 Montesanoc, P. M., Kellyf, R.E. J., Caseyg, K.A., Choudhuryg, B., 2011. A blended global snow

1 product using visible, passive microwave and scatterometer satellite data. *International Journal*
2 *of Remote Sensing*, 32 (5): 1371–1395. doi:10.1080/01431160903548013.

3 Gabellani, S., Silvestro, F., Rudari, R., Boni, G., 2008. General calibration methodology for a
4 combined Horton-SCS infiltration scheme in flash flood modeling, *Nat. Hazards Earth Science.*, 8,
5 1317 - 1327.

6 Gao, Y., Xie, H., Lu, N., Yao, T., Liang, T., 2010. Toward advanced daily cloud-free snow cover
7 and snow water equivalent products from Terra-Aqua MODIS and Aqua AMSR-E measurements. *J*
8 *Hydrol* 385:23–35.

9 Gruhier, C., de Rosnay, P., Hasenauer, S., Holmes, T., de Jeu, R., Kerr, Y., Mougin, E., Njoku, E.,
10 Timouk, F., Wagner, W., and Zribi, M., 2010. Soil moisture active and passive microwave
11 products: intercomparison and evaluation over a Sahelian site. *Hydrol. Earth Syst. Sci.*, 14, 141-156,
12 doi:10.5194/hess-14-141-2010.

13 Han, E., Venkatesh, M. , Heathman, G.C., 2012. Implementation of surface soil moisture data
14 assimilation with watershed scale distributed hydrological model, *Journal of Hydrology*, 416–417,
15 pp. 98–117.

16 Houser, P.R., Shuttleworth, W.J., Famiglietti, J.S., Gupta, H.V., Syed K.H. and Goodrich, D.C.,
17 1998. Integration of soil moisture remote sensing and hydrologic modeling using data assimilation.
18 *Water Resour. Res.*, 34, 3405-3420.

19 Houser, P. R., De Lannoy, G., and Walker, J. P., 2010. Land surface data assimilation in: “Data
20 Assimilation: Making Sense of Observations”. W. Lahoz, B. Khatattov, and R. Menard, Eds.
21 Springer, Netherlands, pp. 549–598.

22 Houser, P.R., De Lannoy, G., Walker, J. P., 2012. Hydrologic Data Assimilation, in: “Approaches
23 to Managing Disaster - Assessing Hazards, Emergencies and Disaster Impacts”. J.P. Tiefenbacher
24 (Ed.). InTech, ISBN: 978-953-51-0294-6, 162 pp.

25 Jackson, T. J., 1980. Profile soil moisture from space measurements, *J. Irrig. Drain. Div.-ASCE*,
26 106, 81–92.

27 Kerr, Y. H., Waldteufel, P., Wigneron, J.-P., Delwart, S., Cabot, F., Boutin, J., et al. 2010. The
28 SMOS mission: New tool for monitoring key elements of the global water cycle. *Proceedings of the*
29 *IEEE*, 98(5), 666–687.

- 1 Kuchment, L. S., Romanov, P., Gelfan, A. N., and Demidov, V. N., 2010. Use of satellite-derived
2 data for characterization of snow cover and simulation of snowmelt runoff through a distributed
3 physically based model of runoff generation, *Hydrol. Earth Syst. Sci.*, 14, 339–350,
4 doi:10.5194/hess-14-339-2010.
- 5 Kumar, S.V., Reichle, R.H., Koster, R.D., Crow, W.T., Peters-Lidard, C.D., 2009. Role of
6 subsurface physics in the assimilation of surface soil moisture observations. *Journal of*
7 *Hydrometeorology*, <http://dx.doi.org/10.1175/2009JHM1134.1>.
- 8 Lakshmivarahan, S. and Lewis, J.M., 2013. Nudging Methods: A Critical Overview, in: “Data
9 Assimilation for Atmospheric, Oceanic and Hydrologic Applications (Vol II)”. Park, Seon Ki, Xu,
10 Liang (Eds.), Chapter 2, , pp 27-58. DOI 10.1007/978-3-642-35088-7 2
- 11 Li, B., Toll, D., Zhan, X., and Cosgrove, B., 2012. Improving estimated soil moisture fields through
12 assimilation of AMSR-E soil moisture retrievals with an ensemble Kalman filter and a mass
13 conservation constraint, *Hydrol. Earth Syst. Sci.*, 16, 105–119, doi:10.5194/hess-16-105-2012.
- 14 Liston, G. E. and Hiemstra, C. A., 2008. A simple data assimilation system for complex snow
15 distributions (SnowAssim), *J. Hydrometeorol.*, 9, 989–1004.
- 16 Liu, Y.Y., Parinussa, R.M., Dorigo, W.A., de Jeu, R.A.M., Wagner, W., van Dijk, A.I.J.M.,
17 McCabe, M.F., Evans, J.P., 2011. Developing an improved soil moisture dataset by blending
18 passive and active microwave satellite-based retrievals. *Hydrol Earth Syst Sci* 15(2):425–436.
19 doi:10.5194/hess-15-425-2011.
- 20 Liu, Y., Weerts, A. H., Clark, M., Hendricks Franssen, H.-J., Kumar, S., Moradkhani, H., Seo, D.-J.,
21 Schwanenberg, D., Smith, P., van Dijk, A. I. J. M., van Velzen, N., He, M., Lee, H., Noh, S. J.,
22 Rakovec, O., and Restrepo, P., 2012. Advancing data assimilation in operational hydrologic
23 forecasting: progresses, challenges, and emerging opportunities, *Hydrol. Earth Syst. Sci.*, 16, 3863-
24 3887, doi:10.5194/hess-16-3863-2012.
- 25 Nash, J. E. and Sutcliffe, J. V., 1970. River flood forecasting through conceptual models I: a
26 discussion of principles, *J. Hydrol.*, 10, 282– 290.
- 27 Njoku, E.G., Jackson, T.J., Lakshmi, V., Chan, T.K., Nghiem, S.V., 2003. Soil moisture retrieval
28 from AMSR-E. *IEEE Trans Geosci Remote Sens* 41:215–229. doi:10.1109/TGRS.2002.808243.

- 1 Parajka, J., V. Naeimi, G. Blöschl, W. Wagner, R. Merz, and K. Scipal (2006), Assimilating
2 scatterometer soil moisture data into conceptual hydrologic models at the regional scale, *Hydrol.*
3 *Earth Syst. Sci.*, 10, 353–368.
- 4 Parinussa, R.M., Holmes, T.R.H., de Jeu, R.A.M., 2012. Soil moisture retrievals from the WindSat
5 spaceborne polarimetric microwave radiometer. *IEEE Trans Geosci Remote Sens.*
6 doi:10.1109/TGRS.2011.2174643.
- 7 Parrens, M., Zakharova, E., Lafont, S., Calvet, J.-C., Kerr, W., Wagner, W., Wigneron J.-P., 2012.
8 Comparing soil moisture retrievals from SMOS and ASCAT over France. – *Hydrol. Earth Syst. Sci.*
9 16, 423–440. www.hydrol-earth-syst-sci.net/16/423/2012/ doi:10.5194/hess-16-423-2012.
- 10 Pauwels, V. R., Hoeben, R., Verhoest, N. E., and De Troch, F. P., 2001. The importance of the
11 spatial patterns of remotely sensed soil moisture in the improvement of discharge predictions for
12 smallscale basins through data assimilation, *J. Hydrol.*, 251, 88–102.
- 13 Pierdicca, N., Pulvirenti, L., Bignami, C., and Ticconi, F., 2013a. Monitoring Soil Moisture in an
14 Agricultural Test Site Using SAR Data: Design and Test of a Pre-Operational Procedure. *IEEE*
15 *Journal of Selected Topics in Applied Earth Observation and Remote Sensing*, 6, 1199-1210.
- 16 Pierdicca, N., Pulvirenti, L., Fascetti, F., Crapolichio R., Talone, M., 2013b. Analysis of two years
17 of ASCAT- and SMOS-derived soil moisture estimates over Europe and North Africa. *European*
18 *Journal of Remote Sensing*, 46, 759-773.
- 19 Pierdicca, N., Pulvirenti, L., and Pace, G., 2014. A Prototype Software Package to Retrieve Soil
20 Moisture From Sentinel-1 Data by Using a Bayesian Multitemporal Algorithm. *IEEE Journal of*
21 *Selected Topics in Applied Earth Observation and Remote Sensing*, 7, 153-166.
- 22 Reichle, R.H., Koster, R.D., Liu, P., Mahanama, S.P.P., Njoku, E.G., Owe, M., 2007. Comparison
23 and assimilation of global soil moisture retrievals from the Advanced Microwave Scanning
24 Radiometer for the Earth Observing System (AMSR-E) and the Scanning Multichannel Microwave
25 Radiometer (SMMR). *J. Geophys Res.* 112:D09108. doi:10.1029/2006JD008033.
- 26 Reichle, R. H., Kumar, S. V., Mahanama, S.P.P., Koster, R. D., and Liu, Q., 2010. Assimilation of
27 Satellite-Derived Skin Temperature Observations into Land Surface Models, *J. Hydrometeorol.*,
28 11, 1103–1122, doi:10.1175/2010JHM1262.1.

- 1 Reichle, R.H., De Lannoy, G.J.M., Forman, B. A., Draper, C.S., Liu, Q., 2013. Connecting Satellite
2 Observations with Water Cycle Variables through Land Data Assimilation: Examples Using the
3 NASA GEOS-5 LDAS. *Surv. Geophys.*. doi:10.1007/s10712-013-9220-8.
- 4 Renzullo, L. J., Dijk, A. I. J. . Van, Perraud, J.-M., Collins, D., Henderson, B., Jin, H., ... McJannet,
5 D. L. (2014). Continental satellite soil moisture data assimilation improves root-zone moisture
6 analysis for water resources assessment. *Journal of Hydrology*, 519, 2747–2762.
7 doi:10.1016/j.jhydrol.2014.08.008
- 8
- 9 Sahoo, A.K., De Lannoy, G.J.M., Reichle, R.H., Houser, P.R., 2013. Assimilation and Downscaling
10 of Satellite Observed Soil Moisture over the Little River Experimental Watershed in Georgia,
11 USA. *Adv. Water Resour.*, 52, 19-33. doi: 10.1016/j.advwatres.2012.08.007.
- 12 Scipal, K., Drusch, M., Wagner, W., 2008. Assimilation of a ERS scatterometer derived soil
13 moisture index in the ECMWF numerical weather prediction system. *Advances in Water Resources*,
14 31(8), 1101-1112. <http://dx.doi.org/10.1016/j.advwatres.2008.04.013>.
- 15 Seneviratne, S.I., Corti, T., Davin, E.L., Hirschi, M., Jaeger, E.B., Lehner, I., Orlowsky, B., Teuling,
16 A.J., 2010. Investigating soil moisture–climate interactions in a changing climate: a review. *Earth
17 Sci Rev* 99:125–161. doi:10.1016/j.earscirev.2010.02.004.
- 18 Silvestro, F., Gabellani, S., Delogu, F., Rudari, R., Boni, G., 2013. Exploiting remote sensing land
19 surface temperature in distributed hydrological modelling: the example of the Continuum model.
20 *Hydrol. Earth Syst. Sci.*, 17, 39-62, doi:10.5194/hess-17-39-2013.
- 21 Stauffer, D.R. and Seaman, N.L., 1990. Use of four-dimensional data assimilation in a limited-area
22 mesoscale model. Part I: Experiments with synoptic-scale data. *Mon. Weather Rev.*, 118, 1250-1277.
- 23 Su, H., Yang, Z.-L., Dickinson, R.E., Wilson, C.R., Niu, G.-Y., 2010. Multisensor snow data
24 assimilation at the continental scale: the value of gravity recovery and climate experiment terrestrial
25 water storage information. *J Geophys Res* 115:D10104. doi:10.1029/2009JD013035.
- 26 Tedesco, M., Narvekar, P.S., 2010. Assessment of the NASA AMSR-E SWE product. *IEEE J Sel
27 Top Appl Earth Obs Remote Sens* 3:141–159.

- 1 USDA Natural Resources Conservation Service (NRCS), National Engineering Handbook (NEH):
2 Part 630 – Hydrology. Chapter 10, July 2004. Available at
3 <http://www.hydrocad.net/neh/630ch10.pdf>
- 4 Wagner, W., Lemoine, G., Rott, H., 1999. A method for estimating soil moisture from ERS
5 scatterometer and soil data. *Remote Sensing Environment* 70: 191-207.
- 6 Wagner, W., Naeimi, V., Scipal, K., de Jeu, R., and Martinez-Fernández, J., 2007. Soil moisture
7 from operational meteorological satellites, *Hydrogeol. J.*, 15, 121–131.
- 8 Wagner, W., Hahn, S., Kidd, R., Melzer, T., Bartalis, Z., Hasenauer, S., Figa, J., de Rosnay, P.,
9 Jann, A., Schneider, S., Komma, J., Kubu, G., Brugger, K., Aubrecht, C., Zuger, J., Gangkofner, U.,
10 Kienberger, S., Brocca, L., Wang, Y., Bloeschl, G., Eitzinger, J., Steinnocher, K., Zeil, P., Rubel, F.,
11 2013. The ASCAT soil moisture product: specifications, validation results, and emerging
12 applications. *Meteorologische Zeitschrift*, 22(1), 5-33, doi:10.1127/0941-
13 2948/2013/0399. <http://dx.doi.org/10.1127/0941-2948/2013/0399>.
- 14 Walker, J.P. and Houser, P.R., 2005. Hydrologic data assimilation. In A. Aswathanarayana (Ed.),
15 *Advances in water science methodologies* (230 pp). The Netherlands, A.A. Balkema.
- 16 Wanders, N., M. F. P. Bierkens, S. M. Jong, A. Roo, and D. Karssenber (2014b), The benefits of
17 using remotely sensed soil moisture in parameter identification of large-scale hydrological models,
18 *Water Resour. Res.*, 50, 6874-6891, doi:10.1002/2013WR014639.
- 19 Weerts, A.H., El Serafy, G.Y.H., 2006. Particle filtering and ensemble Kalman filtering for state
20 updating with hydrological conceptual rainfall–runoff models. *Water Resources Research* 42 (9), 17.